A New Perspective on the Scalar Meson Puzzle, from Spontaneous Chiral Symmetry Breaking Beyond BCS

Pedro J. de A. Bicudo

Departamento de Física and Centro de Física das Interacções Fundamentais, Edifício Ciência, Instituto Superior Técnico,
Av. Rovisco Pais, 1096 Lisboa, Portugal

We introduce coupled channels of Bethe-Salpeter mesons both in the boundstate equation for mesons and in the mass gap equation for chiral symmetry. Consistency is insured by the Ward Identities for axial currents, which preserve the Goldstone boson nature of the pion and prevents a systematic shift of the hadron spectrum. We study the decay of a scalar meson coupled to a pair of pseudoscalars. We also show that coupled channels reduce the breaking of chiral symmetry, with the same Feynman diagrams that appear in the coupling of a scalar meson to a pair of pseudoscalar mesons. Exact calculations are performed in a particular confining quark model, where we find that the groundstate $I = 0$, $^3P_0$ $q\bar{q}$ meson is the $f_0(980)$ with a partial decay width of $40 MeV$. We also find a 30% reduction of the chiral condensate due to coupled channels.

12.39.Kc, 11.30.Rd, 14.40.Cs, 13.25.Jx

I. INTRODUCTION

The Scalar puzzle

The scalar mesons form perhaps the most puzzling family in hadronic physics. The first puzzling fact concerns the experimental errors in the partial decay widths, the decay widths and even the masses. The lightest scalar, $f_0(400 - 1200)$, has a poorly determined mass. The confidence on the decay widths of the $f_0(980)$ and $a_0(980)$ has also decreased [1] strongly since 1994.

The other puzzling argument concerns the matching of the the nine observed states with simple $SU(3)_f$ $q\bar{q}$ states. One would expect four different towers of states corresponding to the two $I = 0$ f_0 (which are not degenerate for instance because the quark s has a clearly larger mass than the quarks u, d) and to the $I = 1$ a_0, and the $I = 1/2$ K_0^*. A short glance at Fig. 1 is sufficient to discard the single light and extremely broad state, the $f_0(400 - 1200)$ as a simple member of this family. Then for the groundstates we could ascribe the narrowest states which are respectively the $a_0(980)$, $K_0^*(1430)$, $f_0(980)$ and $f_0(1500)$, and for the radial excited states we could respectively ascribe the $a_0(1450)$, $K_0^*(1950)$, $f_0(1370)$ and $f_0(2200)$. However the decay widths Γ of the groundstate scalars are narrower than expected when compared with other resonances decaying in the same pseudoscalar pairs but with higher angular momentum, except for the only precisely measured one, the $K_0^*(1430)$. Moreover

the breaking of $SU(3)_f$ due to the $m_u \simeq m_d << m_s$ mass difference is nearly the double than expected when compared with the vector meson family and with most baryons. This is only comparable with the splittings in the pseudoscalar family.
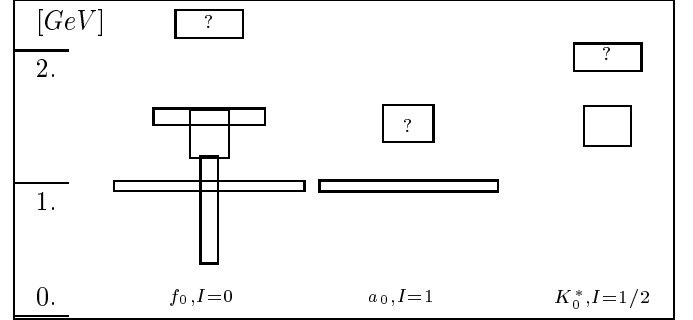

FIG. 1. We represent, with rectangles of height Γ, the experimentally observed scalar resonances according to the Review of Particle Properties, and mark the unconfirmed ones with a "?". In a naive quark model, the a_0 and K_0^* channels should show half of the resonances of the f_0 channel.

The scalar family is also the most interesting place to search for the lightest (S-wave) non $q\bar{q}$ states. There are several theoretical candidates to extra states which may be found. The lightest glueball, which is expected from QCD, should be a scalar [2]. The model of Isgur and Weinstein et al [3] suggests that the narrowest scalars are meson-meson molecules. The One Meson Exchange Potential models for the NN interaction usually postulates a scalar meson σ with a light $M \simeq 0.5 GeV$. In strongly coupled effective meson models [4,5], extra poles appear in the S matrix when couplings are large. These meson models turn out to be the most successful models ones so far, explaining with complex nonlinear effects not only the narrow $a_0(980)$ and $f_0(980)$ which are due to the vicinity of the KK threshold, but also the very wide and light $f_0(400 - 1200)$.

The relevance of chiral symmetry breaking

Chiral symmetry breaking is important for the study of scalar mesons and their decays for several reasons. Unlike the vector, axial and tensor mesons, the scalar and pseudoscalar mesons are mixed by the chiral rotations,

$$\bar{\psi}\psi \rightarrow \cos(\theta)\bar{\psi}\psi + i\sin(\theta)\bar{\psi}\gamma_5\psi$$
$$\bar{\psi}\gamma_5\psi \rightarrow -i\sin(\theta)\bar{\psi}\psi + \cos(\theta)\bar{\psi}\gamma_5\psi , \tag{1}$$

thus scalars and pseudoscalars are particularly sensitive to the chiral symmetry. The very small mass of the pseudoscalars is usually explained with chiral symmetry breaking. Moreover, since scalars decay essentially in pseudoscalars, the pseudoscalar mass is important for the scalar decay. Thus we expect that not only the pseudoscalar mesons but also the scalars must contain the signature of the breaking of chiral symmetry. Inversely, the breaking of chiral symmetry is generated from the trivial vacuum by scalar condensation, and we also expect that the scalar properties should affect the breaking of chiral symmetry.

These effect have been studied in phenomenological meson sigma models, see for instance [5]. At the more microscopic level of quarks, Dynamical Spontaneous Chiral Symmetry Breaking (χSB) has been worked out in the past with several different quark-quark effective interactions, at the same level as Bardeen Cooper and Schrieffer (BCS) did [6] for Superconductivity. Since [7] Nambu and Jona-Lasinio (NJL) and until recently [8,9] the mass gap equation in chiral physics has been so far of the BCS type, [7] including only the first order contribution from the quark-quark interaction. In this case the quark condensate consists [10] of scalar $^3P_0$ quark antiquark pairs. At the BCS level, which is very consistent, it is possible to derive the mass gap equation in several different but equivalent methods. The pseudoscalar meson properties have been studied in great detail and the full meson spectrum has been also been calculated in the literature [11]. However the BCS approach is not exact in the case where coupled channels of mesons are included.

Coupled Channels of Mesonic $q\bar{q}$ pairs

In the case of weak coupled channel effects, it would be acceptable to start from boundstates obtained at the BCS level and couple them with the help of the annihilation diagrams of Fig. 2, without changing the mass gap equation. In this sense we started some years ago to develop a program [12] to study the coupled channel effects in quark models with chiral symmetry breaking.
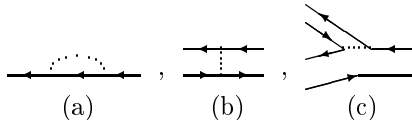

FIG. 2. We show the quartic diagrams which may contribute to the boundstate equation. In the strong coupling BCS, (a) is included in the self energy and (b) is included in the interaction kernel. Diagram (c) which creates or annihilates quark-antiquark pairs is only used in what we call beyond BCS.

The first result of our program was to reproduce [12] at the BCS level the strong decay of the vector meson ρ (and of the ϕ). This has been studied by other authors recently [13]. Later we extended our program to

the nucleon interactions and had good results [12] in the K_N s-wave scattering, the $F_{N\pi N}$ and $F_{N\pi\Delta}$ derivative couplings and the $N\,N$ short range interaction.

However there is a recent trend in the literature to reevaluate coupled channel effects in many hadronic phenomena. Some years ago they were not supposed to account for more than 10% of a hadron mass but presently they are supposed to contribute with a negative mass shift of the order of 50% of the bare mass [14–16].

Moreover it is possible to prove that the vacuum solution of the BCS mass gap equation is not exact when coupled channels are included. Suppose that the mass gap equation for chiral symmetry breaking was solved at the BCS level, i.e. without including the coupled channels, then a bare pion with vanishing bare mass would be found. If the coupled channels were then included, at posteriori, in the bound state equation then the pion mass would be the sum of the small bare mass plus a mass shift and thus would have a resulting nonvanishing mass, which implies that the pion lost its Goldstone boson nature. This result is unavoidable, and can be proved variationally. Thus the mass gap should be solved beyond BCS, especially when scalar mesons are studied.

Solving this problem is a corner stone of our program. It amounts to join the BCS mechanism with the mean field expansion of effective mesons.The logical path of the method we will follow is illustrated in Fig. 3. Self consistency is insured by Ward Identities, and the scalar-pseudoscalar coupling will turn out to be crucial for this development. The reward of solving chiral symmetry breaking with coupled channels is a π with a vanishing positive mass in the chiral limit complying with all the theorems of PCAC, and a tower of resonances (including the scalar meson resonances) above the π with higher masses due to radial, angular, or spin excitations. In particular the resonances also have an imaginary component of the mass $\frac{-i\Gamma}{2}$ that describes the decay width into the open channels.
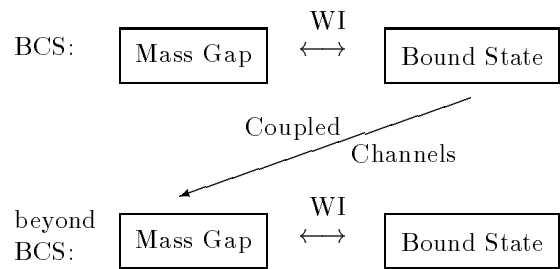

FIG. 3. We illustrate the principle which is followed in this paper to include the coupled channels in the mass gap equation

The paper

The aim of this paper is to study at the quark level some meson decays which were studied in the literature without including directly the full quark contributions

[4,5]. We specialize in the groundstate $f_0 \rightarrow \pi \pi$ decay. We also study the effect of the meson coupled channels on the quark condensed vacuum.

The remaining of this paper is organized as follows. In section II we review the scalar masses and decays at the BCS level. This includes the choice of an effective interaction for quarks, the mass gap equation and the Bethe Salpeter equation at the BCS level, the scalar coupling to pseudoscalars, and the scalar decays width. In Section III we produce a finite extension beyond BCS for a class of confining effective interactions, derive the mass gap equation with coupled channels, link it to the scalar-pseudoscalars coupling, and solve the mass gap equation. Results are shown in Section IV together with their discussion. We also include 4 appendices.

II. THE BCS LEVEL FOR A PARTICULAR FORMALISM

A. The choice of an effective interaction

The quantitative results of this paper will be obtained with a particular chiral invariant strong potential which is an extended version of the NJL potential [7]. For the study of dynamical χSB it is crucial to have a closed model where calculations can be carried until the end, because precise cancellations occur. At this point we abandon the explicit SU(3) gauge invariance. We start by introducing a class [11,17] of Dirac quark Hamiltonians which are, in the limit of massless quarks, explicitly chiral invariant,

$$H = \int d^3x \left[\psi^\dagger(x) \left(m_0\beta - i\vec{\alpha} \cdot \vec{\nabla} \right) \psi(x) + \sum_l \frac{1}{2} \overline{\psi}(x)\Omega_l\psi(x) \int d^4y \ V_l(x-y) \ \overline{\psi}(y)\Omega_l 2\psi(y) \right] \quad (2)$$

The quark-quark interaction, is an effective color dependent 2-body interaction. In eq. (2) the operators Ω_l include both the color Gell-Mann matrices and the Dirac matrices. The sum in the Dirac matrices must be chiral invariant. Because the Gell-Mann matrices are traceless there will be no tadpoles in this scheme. In Hadronic Physics the effective interaction should be simultaneously color confining, in the Minkowsky space, local, and Lorentz invariant. However no interaction which complies with all these constraints has yet been used to study chiral symmetry breaking.

The models used in the literature divide essentially in two classes, in particular the more popular one springs directly from NJL [7], is Euclidean and due to the structure of the interaction has usually no analytic continuation to the Minkowsky space and lacks confinement. This class has been extended in many different directions. For instance finite size boundstates were included with the Global Color Model of ref. [18], and a sophisticated interaction with a general tensor structure, an almost linear long range and pertubative short range is found in ref. [19].

The other class of models [10,11,20] has the single drawback of using an instantaneous potential (except for Lorentz invariant extensions [21] of this class). But it has the advantage of being confining which allows to study the whole [11,12,17,22–24] hadron spectrum. This approximation also has the advantage to allow a straightforward application to low energy nuclear physics. For the theoretical foundations of these models, including the connection to both pertubative and nonpertubative QCD, see [25].

Thus we choose to calculate the quantitative results of this paper within the second class of Nambu and Jona-Lasinio potentials. We use a simple model which is in very good agreement with the experiments in what concerns the hadronic spectroscopy, the decays of the vector mesons ρ and Φ, the coupling of a π to a N or Δ and the N N short range interaction [12], moreover it supports that chiral symmetry breaking is very stable in the presence of Nuclear Matter [24]. While confinement is an essential physical aspect of the model, the instantaneous approximation simplifies drastically the energy dependence of the interaction, and allows to work in a framework which is familiar to Schrödinger's equations. The 2-body potential for Dirac quarks is,

$$\frac{-3}{4} \frac{\vec{\lambda}}{2} \cdot \otimes \frac{\vec{\lambda}}{2} \left[\gamma_0 \otimes \gamma_0 \left(k_0^3 r^2 - U \right) + a\vec{\gamma} \cdot \otimes \vec{\gamma} k_0^3 r^2 \right] \delta(t) \quad (3)$$

and the Fourier transform of the potential is,

$$\Omega_l \widetilde{V}_l(k) \otimes \Omega_l = \frac{-3}{4} \frac{\vec{\lambda}}{2} \cdot \otimes \frac{\vec{\lambda}}{2} \left[\gamma_0 \otimes \gamma_0 \left(-K_0^3\Delta_k - U \right) + a\vec{\gamma} \cdot \otimes \vec{\gamma} \left(-K_0^3\Delta_k \right) \right] (2\pi)^3\delta^3(k) \ , \quad (4)$$

where we dropped the sum in color and Dirac indices. The factor $-3/4$ simplifies the color contribution for color singlets.
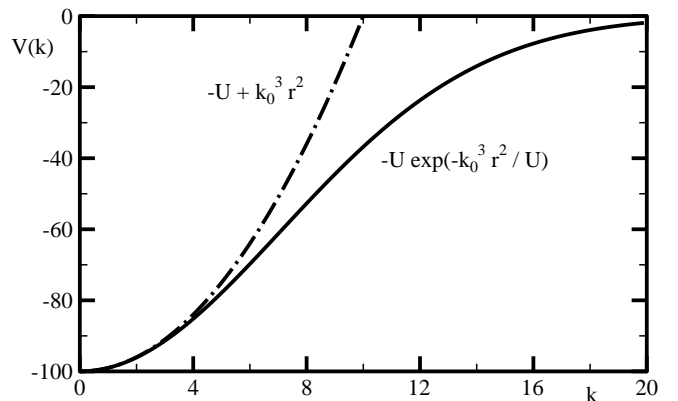

FIG. 4. $-Ue^{\frac{-k_0^3 r^2}{U}}$ is an example of a potential which tends to $-U + k_0^3 r^2$ in the limit of infinite U. We illustrate this in the case where $K_0 = 1$, $U = 100$.

3

The $\gamma_0 \cdot \gamma_0$ term in the potential is the limit of a series of attractive potentials, see Fig. 4, and U is an arbitrarily large infrared constant. The infinite U reappears in the self energy and in color singlet channels this cancels the infinitely attractive potential. Any colored state will have a mass proportional to U and will thus be confined, see appendix A.

The choice of an harmonic potential is not crucial, a linear [20] or funnel potential has also been used, but a quadratic form is simpler. In the case of light quarks the current quark mass m_0 is almost vanishing and it essentially affects the family of the π which is a quasi Goldstone boson.

The $\vec{\gamma} \cdot \vec{\gamma}$ term is introduced in order to have Lorentz invariant pions which are relativistic in the scalar decay. Clearly the wrong result of a simple $\gamma_0 \otimes \gamma_0$ instantaneous interaction is the constant f_π which is quite small and is not Lorentz invariant. The hope to cure f_π with covariant extensions of the model turned out to fail since they merely [21] increased f_π in 30%. The value for the parameter a which renders the pion Lorentz invariant is $a = -.18$, and for most calculations (except for f_π which is increased by 300%, see subsection D) this a yields a result comparable to the one we had for $a = 0$. The small a suggests that the cure of f_π may be related with the pertubative short range [25] quark-quark interaction .

Once a is fixed, this model has the single scale of the oscillator parameter K_0. The simplest adimensional units of $K_0 = 1$ will be used from now on in computations. When comparing with experiments we will rescale K_0 to the value of $K_0 = 330\,MeV$ which gives the best overall fit of the meson spectrum. We will also work in the momentum representation and drop the tilde $\tilde{\ }$ from the potential.

B. Chiral Symmetry Breaking at the BCS level with quarks and antiquarks

At the BCS level and with a color dependent interaction the Schwinger Dyson equation for the quark self energy (which is also the mass gap equation) is,

$$\longrightarrow^{-1} = \mathcal{S}_0^{-1} - \overset{\cdot\cdot\cdot}{\cdots}$$
$$\mathcal{S}^{-1} = -i\,\not{p} - \Sigma \qquad (5)$$

where the full (up to the approximation which is chosen) propagator $\mathcal{S}$ is denoted as usual by $\longrightarrow$. The subindex $_0$ is reserved for the free functions. The effective quark-quark 2-body interaction of eq. (2), a chiral invariant and color dependent interaction, is represented with a dotted line ……. The Bethe Salpeter equation for the vertex is related by the Ward Identities with eq.(5), see Appendice C,

$$\bullet\!\!\!\!- = \Gamma_0 + \overset{\vdots}{\rhd}\!\!-$$

$$\Gamma(p,q) = \Gamma_0 + \int \frac{d^4k}{(2\pi)^4} V(k)\Omega S(p+k)$$
$$\Gamma(p+k,q+k)S(q+k)\Omega \qquad (6)$$

where the full vertex Γ^μ is denoted by $\bullet\!\!-$. When eq.(6) is iterated, we find that it includes, the Bethe-Salpeter ladder, which will be represented diagrammatically by a box with 4 emerging lines $=\square=$,

$$\text{(diagram)} \qquad (7)$$

where the ladder represents the mesons, see Appendice C. In this way the quark propagator, the vertices and the mesons are intertwined.

In this case of an instantaneous interaction, it is convenient to substitute the Dirac fermions in terms of Weyl fermions, in order to find the hadron spectrum. The Dirac propagator can be decomposed in a quark propagator and an antiquark propagator, moving both forward in time.

$$\mathcal{S}_{Dirac}(k_0, \vec{k}) = \frac{i}{\not{k} - m + i\epsilon}$$
$$= \frac{i}{k_0 - E + i\epsilon} \frac{1 + \frac{m}{E}\beta + \frac{k}{E}\vec{\alpha}\cdot\hat{k}}{2}\beta$$
$$- \frac{i}{-k_0 - E + i\epsilon} \frac{1 - \frac{m}{E}\beta - \frac{k}{E}\vec{\alpha}\cdot\hat{k}}{2}\beta \qquad (8)$$

It is convenient to use [11,10] the quark energy projectors,

$$\Lambda^+ = \frac{1}{2}\left(1 + S\beta + C\hat{k}\cdot\vec{\alpha}\right) = \sum_s u_s u_s^\dagger,$$
$$\Lambda^- = \frac{1}{2}\left(1 - S\beta - C\hat{k}\cdot\vec{\alpha}\right) = \sum_s v_s v_s^\dagger, \qquad (9)$$

where $S = \sin(\varphi) = \frac{m}{E}$, $C = \cos(\varphi) = \frac{k}{E}$ and φ is a chiral angle which in the non condensed case is equal to $\arctan\frac{m_0}{k}$, (m_0 is the current mass of the quark) but is not determined from the onset when chiral symmetry breaking occurs. In this case the physical quark mass is a variational function $m = m(k)$ which is determined by the mass gap equation. This is equivalent to use the chiral angle $\varphi = \varphi(k)$ as the variational function. In Fig. 5 we show examples of non trivial solutions for the function $\varphi(k)$.

The energy projectors can be decomposed in the quark spinor $u(k)$ and in the antiquark spinor $v(k)$,

$$u_s(\mathbf{k}) = \frac{\Lambda^-}{\sqrt{\frac{1+S}{2}}} u_s(0) = \left[\sqrt{\frac{1+S}{2}} + \sqrt{\frac{1-S}{2}}\hat{k}\cdot\vec{\alpha}\right] u_s(0)$$

$$v_s(\mathbf{k}) = \frac{\Lambda^-}{\sqrt{\frac{1+S}{2}}} v_s(0) = \left[\sqrt{\frac{1+S}{2}} - \sqrt{\frac{1-S}{2}}\hat{k}\cdot\vec{\alpha}\right] v_s(0)$$

$$= -i\sigma_2\gamma_5 u_s^*(\mathbf{k}) . \qquad (10)$$

And finally the Dirac quark propagator is decomposed in,

$$\mathcal{S}_{Dirac}(w, \vec{k}) = u(k)\mathcal{S}_q(p_0, \vec{k})u^\dagger(k)\beta$$
$$-v^\dagger(k)\mathcal{S}_{\bar{q}}(-p_0, -\vec{k})v(k)\beta \, , \qquad (11)$$

where the quark and antiquark Weyl propagators are.

$$\mathcal{S}_q(w, \vec{k}) = \mathcal{S}_{\bar{q}}(w, \vec{k}) = \frac{i}{w - E(k) + i\epsilon} \, . \qquad (12)$$

The quark and antiquark formalism is convenient to calculate the hadron spectroscopy. With Weyl propagators the BS equation simplifies into the Salpeter equation, in a form which is as close as possible to the more intuitive Schrödinger equation. In the Feynman rules with Weyl propagators, we choose to redefine the vertices of the effective potential which now include the spinors $u^\dagger$, u, $v^\dagger$ and v. The "$-$" sign which affects the antiquark propagator in eq.(11) could also be included in the vertices with $v^\dagger$, but we prefer to recover the equivalent rules which are common to nonrelativistic field theory. This "$-$" sign together with the one from the fermion loops will be included in the antiquark vertex and in diagrams with quark exchange or with antiquark exchange. The Dirac vertex γ_0 is now replaced by $u^\dagger u$, $u^\dagger v$, $v^\dagger u$ or $-v^\dagger v$ when the vertex is respectively connected to a quark, a pair creation, a pair annihilation or an antiquark; and the Dirac vertex $\vec{\gamma}$ is respectively replaced by $u^\dagger \vec{\alpha} u$, $u^\dagger \vec{\alpha} v$, $v^\dagger \vec{\alpha} u$ or $-v^\dagger \vec{\alpha} v$. We choose the graphical notation for the Weyl propagators of quarks and antiquarks,

$$\mathcal{S}_{Dirac}(w, \vec{k}) = \overset{w, \vec{k}}{\underleftarrow{\quad}} D \, ,$$

$$\mathcal{S}_q(w, \vec{k}) = \overset{w, \vec{k}}{\underleftarrow{\quad}} \quad , \quad \mathcal{S}_{\bar{q}}(-w, -\vec{k}) = \overset{w, \vec{k}}{\underrightarrow{\quad}} \qquad (13)$$

where the Diagrams using the Feynman rules corresponding to the Dirac fermion propagators will have a subindex D in the remaining of the paper. In the case of the Weyl propagators (which will be used more often the the Dirac propagators) the quark will be represented with an arrow pointing to the left while the arrow pointing to the right represents an antiquark (both move forward in the time direction).

C. The BCS mass gap equation and the quark energy

Here we derive the mass gap equation, and the quark dispersion relation, replacing the propagator of eq. 11 in the Schwinger Dyson equation for the quark self energy (5),

$$u \overset{}{\underleftarrow{}}_{w, \vec{k}}^{-1} u^\dagger - v \overset{}{\underrightarrow{}}_{w, \vec{k}}^{-1} v^\dagger = \beta \frac{\not{k} - m_0}{i} - \beta \, \overset{\cdots}{\underleftarrow{}}_D \quad (14)$$

Another equivalent method is to use the Hamiltonian formalism for the quark and antiquark creators and annihilators [10], and find the Bogoliubov Valatin transformation which would minimize the vacuum energy density.

In that Hamiltonian formalism the mass gap equation is also obtained when the quark antiquark pair creation operators are postulated to vanish in the Hamiltonian, in order to ensure the vacuum stability against spontaneous generation of scalars. With the present method we project eq(14) with the spinors $u^\dagger \cdots u$ and $u^\dagger \cdots v$, and we get directly the quark and antiquark energy and the mass gap equation,

$$E(k) = u_s^\dagger(k)\left\{ k\hat{k} \cdot \vec{\alpha} + m_0\beta - \int \frac{dw'}{2\pi}\frac{d^3k'}{(2\pi)^3}iV_l(k - k') \right.$$
$$\left. \left[\frac{\Omega_l\Lambda^+(k')\Omega_l}{w' - E(k') + i\epsilon} - \frac{\Omega_l\Lambda^-(k')\Omega_l}{-w' - E(k') + i\epsilon} \right] \right\} u_s(k),$$
$$0 = u_s^\dagger(k)\left\{ k\hat{k} \cdot \vec{\alpha} + m_0\beta - \int \frac{dw'}{2\pi}\frac{d^3k'}{(2\pi)^3}iV(k - k') \right.$$
$$\left. \left[\frac{\Omega_l\Lambda^+(k')\Omega_l}{w' - E(k') + i\epsilon} - \frac{\Omega_l\Lambda^-(k')\Omega_l}{-w' - E(k') + i\epsilon} \right] \right\} v_{s''}(k). \quad (15)$$

In the case of an instantaneous interaction, the loop integral in the energy w removes the pole in the propagator,

$$\int \frac{dw}{2\pi}\frac{i}{w - E(k) + i\epsilon} = \frac{1}{2} \qquad (16)$$

and in the case of a quadratic interaction, the loop integral in the momentum is transformed in a Laplacian, see eq.(4). Some useful properties are,

$$u_s^\dagger u_{s'} = 1\delta_{ss'} \quad , \quad u_s^\dagger v_{s'} = 0 \left[\vec{\sigma} \cdot \hat{k}i\sigma_2\right]_{ss'}$$
$$u_s^\dagger \beta u_{s'} = S\delta_{ss'} \quad , \quad u_s^\dagger \beta v_{s'} = -C\left[\vec{\sigma} \cdot \hat{k}i\sigma_2\right]_{ss'} \quad (17)$$
$$u_s^\dagger \vec{\alpha} \cdot \hat{k}u_{s'} = C\delta_{ss'} \quad , \quad u_s^\dagger \vec{\alpha} \cdot \hat{k}v_{s'} = S\left[\vec{\sigma} \cdot \hat{k}i\sigma_2\right]_{ss'}$$
$$u_s^\dagger \beta\vec{\alpha} \cdot \hat{k}u_{s'} = 0\delta_{ss'} \quad , \quad u_s^\dagger \beta\vec{\alpha} \cdot \hat{k}v_{s'} = 1\left[\vec{\sigma} \cdot \hat{k}i\sigma_2\right]_{ss'} .$$

We get finally for the quark energy,

$$E(k) = kC + m_0S + \frac{1}{2}\left[+S\Delta(S) + C\hat{k} \cdot \Delta(\hat{k}C)\right] + \frac{U}{2}$$
$$+a\frac{1}{2}\left[-3S\Delta(S) - C\hat{k} \cdot \Delta(\hat{k}C)\right]$$
$$= \frac{U}{2} + kC + m_0S - \frac{\dot{\varphi}^2}{2} - \frac{C^2}{k^2}$$
$$-a\left[SC\Delta\varphi - \frac{C^2}{k^2} - \left(S^2 + \frac{1}{2}\right)\dot{\varphi}^2\right] , \qquad (18)$$

where in color singlets the $U/2$ term will cancel the $-U$ term from the 2-body quark potential. For the mass gap equation we get,

$$0 = \left\{ kS - m_0C + \frac{1}{2}\left[-C\Delta(S) + S\hat{k} \cdot \Delta(\hat{k}C)\right] \right.$$
$$\left. +a\frac{1}{2}\left[+3C\Delta(S) - S\hat{k} \cdot \Delta(\hat{k}C)\right] \right\}\left[\vec{\sigma} \cdot \hat{k}i\sigma_2\right]_{ss'}$$
$$= -\Delta\varphi + 2kS - 2m_0C - \frac{2SC}{k^2}$$
$$-a\left[-\left(2C^2 + 1\right)\Delta\varphi + 2SC\left(\dot{\varphi}^2 - \frac{1}{k^2}\right)\right] . \qquad (19)$$

The mass gap equation is in general a nonlinear integral equation, but in this case of a harmonic potential it simplifies to a differential equation. We solve it numerically with the Runge-Kutta and shooting method, see Fig. 5 for the solution.
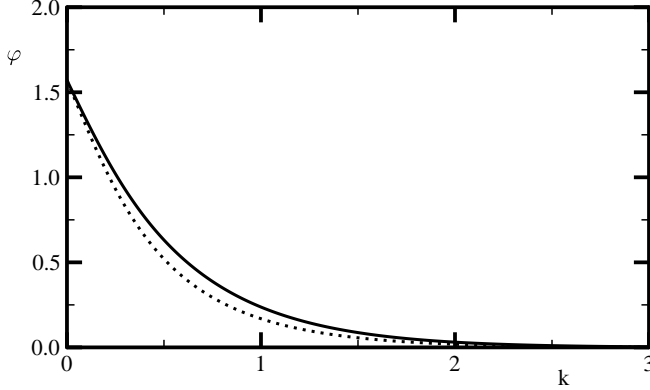

FIG. 5. We show the BCS chiral angle in units of $K_0 = 1$. We also represent with a doted line the chiral angle that we obtain going beyond BCS.

D. The pseudoscalar and scalar solutions to the Salpeter equation

The homogeneous Salpeter equation for a meson (a color singlet quark antiquark boundstate) is, according to Appendix C,

$$\frac{+M(P)-E(k_1)-E(k_2)}{i}\phi^+(k,P) = -iu^\dagger(k_1)\chi(k,P)v(k_2)$$
$$\frac{-M(P)-E(k_1)-E(k_2)}{i}\phi^{-t}(k,P) = -iv^\dagger(k_1)\chi(k,P)u(k_2)$$
$$\chi(k,P) = \int \frac{d^3k'}{(2\pi)^3}\; V_l(k-k')\Omega_l \left(u(k_1')\phi^+(k',P)v^\dagger(k_2')\right.$$
$$\left. +v(k_1')\phi^{-t}(k',P)u^\dagger(k_2')\right)\Omega_l \quad (20)$$

where $k_1 = k + \frac{P}{2}$, $k_2 = k - \frac{P}{2}$ and P is the total momentum of the meson. We use the Bethe-Salpeter amplitude χ as an intermediate step to compute the contribution of interaction V to the boundstate equation. The wave functions ϕ^+ and ϕ^- are equivalent to the Bethe-Salpeter amplitude χ . For color singlets the contribution of the infinite infrared constant U cancels, see Appendix A. The equation is also flavor independent, and we will now concentrate on the *momentum $\otimes$ spin* part of the wave-functions. We will now drop the U term and the color dependence from the equations. In this section the matrices Ω_l will only include the Dirac structure, $\Omega_l \otimes \Omega_l = \gamma_0 \otimes \gamma_0 + a\vec{\gamma}\cdot\otimes\vec{\gamma}$. With the aim of studying the f_0 decay in a pair of π, we will now solve the bound state equation equation for the scalar f_0 in its center of mass frame and the equation for the pseudoscalar groundstate π in the limit of small P and in the limit of large P.

Due to the large mass of the scalar meson f_0 in this model, it turns out that the negative energy ϕ^- component for the groundstate is less than 10% of the positive

energy component ϕ^+. The Schrödinger limit, where only the positive energy component is considered, is therefore acceptable. A general form for the $^3P_0$ wave-function for the scalar is

$$\phi^+(k)_{s_1 s_2} = k\phi_s(k)\frac{[\vec{\sigma}\cdot\hat{k}i\sigma_2]_{s_1 s_2}}{\sqrt{2}} \quad (21)$$

the truncated BS amplitude is then,

$$\chi_s = -\Omega_l\Delta\frac{2k\phi_s(k)}{1+S}\Lambda^+u_{s_1}(0)\frac{[\vec{\sigma}\cdot\hat{k}i\sigma_2]_{s_1 s_2}}{\sqrt{2}}v_{s_2}^\dagger(0)\Lambda^-\Omega_l$$
$$= \Omega_l\Delta\frac{\Lambda^+\beta\vec{\alpha}\cdot\vec{k}\phi_s(k)}{\sqrt{2}}\Omega_l \;, \quad (22)$$

we get for left hand side of eq. (20) ,

$$u^\dagger(k)\chi(k,0)v(k) = \frac{1+a}{2}\Delta\left(\phi^+\right)+\frac{1-a}{2}S\Delta\left(S\phi^+\right)$$
$$+\frac{1-3a}{2}C\Delta\left(C\phi^+\right)+\frac{1-3a}{k^2}C^2\phi^+ \quad (23)$$

and the radial Salpeter equation for the scalar in the center of mass is,

$$\left[2E(k)-M-\left(\frac{d^2}{dk^2}-\frac{2}{k^2}-\frac{\dot{\varphi}^2}{2}+\frac{C^2}{k^2}\right)-a\left(-C^2\frac{d^2}{dk^2}\right.\right.$$
$$\left.\left.+2SC\varphi\frac{d}{dk}-\frac{C^2}{k^2}+SC\ddot{\varphi}+\frac{1+2C^2}{2}\dot{\varphi}^2\right)\right]k^2\phi_s = 0 \quad (24)$$

Solving the bound state equation we find that the solution of the equation is very close to a Gaussian,

$$\phi_s(k) \simeq \frac{e^{\frac{-k^2}{2\alpha_s^2}}}{\mathcal{N}_s} \;,\; \mathcal{N}_s^{-1} = \frac{4\sqrt{\pi\sqrt{\pi}}}{\sqrt{3}\alpha_s^{5/2}} \;,\; \alpha_s \simeq .476 \quad (25)$$

and the mass is $M = 2.94\,K_0 = 970\,MeV$ which is close to the most probable experimental mass of the f_0 groundstate.

We now study the pseudoscalar groundstate in the low P limit, which was already studied extensively in the literature [11,12]. For vanishing P we find that $\phi^+ = -\phi^-$ and both are proportional to $\sin(\varphi)$. This is due to the Goldstone boson nature of the π, see the result of Appendix C. However this component of the wavefunction has zero norm, and it is necessary to include the next order of the expansion in P to determine the norm. The most general low P pseudoscalar wave-function is then,

$$\phi^+ = \mathcal{N}_p^{-1}\left(S+\frac{M(P)}{k}f_1+ig_1\frac{\vec{P}}{k}\cdot\hat{k}\times\vec{\sigma}\right)\frac{i\sigma_2}{\sqrt{2}}$$
$$\phi^- = \mathcal{N}_p^{-1}\left(-S+\frac{M(P)}{k}f_1-ig_1\frac{\vec{P}}{k}\cdot\hat{k}\times\vec{\sigma}\right)\frac{i\sigma_2}{\sqrt{2}}, \quad (26)$$

where the norm is a function of the π energy,

$$\mathcal{N}_p^2 = \left(2f_\pi^{(t)}\right)^2 M \;\;,\;\; M^2(P) = M^2(0) + P^2\sqrt{\frac{f_\pi^{(s)}}{f_\pi^{(t)}}}$$

$$M^2(0) = -\frac{2m_0\langle\bar\psi\,\psi\rangle}{f_\pi^{(t)2}} \;\;,\;\; \langle\bar\psi\,\psi\rangle = -6\int\frac{d^3k}{(2\pi)^3}S \quad (27)$$

and where in the case of an instantaneous interaction there are [11,12] usually 2 different $f_\pi^{(t)}$ and $f_\pi^{(s)}$,

$$f_\pi^{(t)} = \sqrt{\frac{3}{\pi^2}\int_0^\infty dk\; k f_1 S} \qquad (28)$$

$$\sqrt{f_\pi^{(s)}f_\pi^{(t)}} = \sqrt{\frac{1}{2\pi^2}\int_0^\infty dk\; -k^2 S\dot\varphi + 4kC(g_1+1/2)}\,.$$

Substituting the wave-functions of eq. (26) in eq. (20), and expanding the resulting equation up to the first order in P, we get the equations for the f_1 and g_1 components,

$$\ddot f_1 = \frac{1}{1+a(2S^2+1)}\Big[-kS+(2Ck)f_1$$
$$+4a\left(-SC\Delta\varphi - C^2/k^2 + S^2\dot\varphi^2 + \dot\varphi^2/2\right)f_1$$
$$-4aSC\dot\varphi(\dot f_1 - f_1/k)\Big], \qquad (29)$$

$$\ddot g_1 = \frac{1}{1+a(2S^2-1)}\Big[kC+(2kC+2S^2/k^2)g_1$$
$$+2a(S^2/k^2 - 2SC\Delta\varphi - 2S^2\dot\varphi^2)g_1$$
$$-4aSC\dot\varphi(\dot g_1 - g_1/k)\Big]. \qquad (30)$$

It turns out that the parameter a has little effect on most functions, except for f_1. The homogeneous equation for f_1 has the solution $a_0 = -.195$ an thus $f_1 \alpha 1/a - a_0$. This will essentially affect $f_\pi^{(t)}$, $f_\pi^{(s)}$ and the pion velocity c. We find for $a \simeq -.18$ that $c = 1$, $f_\pi^{(t)} = f_\pi^{(s)} = 0.21K_0 \simeq 69\,MeV$. This shows a clear improvement of the model, with a correct relativistic pion and a better f_π.
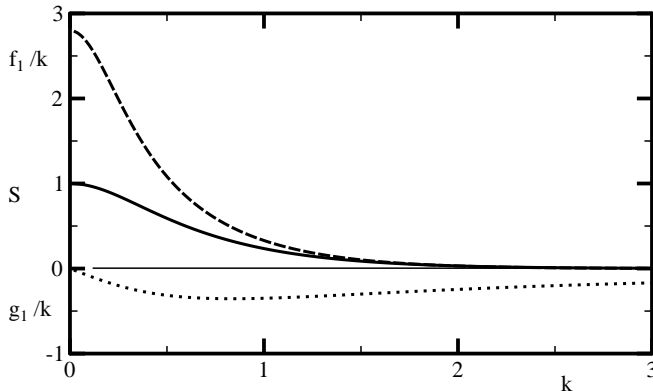

FIG. 6.   We represent the π wave-functions functions S, f_1/k and g_1/k respectively with solid, dashed and dotted lines, in the adimensional units $K_0 = 1$.

We now discuss the pseudoscalar groundstate in the other limit of large momentum P. In this case the negative energy components are suppressed by a factor of $1/P$. The chiral angle φ, depicted in Fig. [5] vanishes completely, and the spinors are simpler, for instance,

$$u_s(k_1) \simeq \frac{1+\vec\alpha\cdot\hat k_1}{\sqrt 2}u_s(0)\;,\; \hat k_1 \simeq \hat P + \frac{2}{P}\vec k_\perp \qquad (31)$$

where the index $\perp$ denotes the projection $\vec k - (\vec k\cdot\widehat P)\widehat P$ of a vector $\vec k$ in the plane perpendicular to $\vec P$. The vertices, up to first order in $1/P$ are for instance,

$$u_s^\dagger(k_1)u_{s'}(k_1') \simeq \delta_{ss'} - \frac{1}{P}i\vec\sigma_{ss'}\hat P\times(\vec k_\perp - \vec k_\perp') \qquad (32)$$

$$u_s^\dagger(k_1)\vec\alpha u_{s'}(k_1') \simeq \hat P\delta_{ss'} + \frac{(\vec k_\perp + \vec k_\perp') + i\vec\sigma\times(\vec k_\perp - \vec k_\perp')}{P}$$

Up to first order in $2/P$ the equation for positive and negative energy boundstate functions $\phi^\pm(k)i\sigma_2/_{\sqrt 2}$ is,

$$0 \simeq \left(P + \frac{2k^2}{P} \mp M - (1-a)\Delta_k\right)\phi^\pm(k)$$
$$-2i(1-a)\frac{\widehat P}{P}\times\vec\nabla_k\cdot\left\{\vec\sigma,\phi^\pm(k)\right\}$$
$$-a\Delta_k\phi^\mp(k) - \frac{2}{P^2}\vec\sigma_\perp\cdot\phi^\mp(k)\vec\sigma_\perp \qquad (33)$$

We find that the wave-function has a component with structure $i\vec\sigma\cdot\widehat P\times\vec k$. However this component is smaller than the s-wave component by a factor of less than $1/P$. Thus we find that the *momentum $\otimes$ spin* solution up to highest order in, is essentially a positive energy Gaussian function $\phi_p(k)\frac{i\sigma_2}{\sqrt 2}$,

$$\phi_p(k) \simeq \frac{e^{\frac{-k^2}{2\alpha_p^2}}}{\mathcal{N}_p}, \; \mathcal{N}_p^{-1} = \left(\frac{2\sqrt\pi}{\alpha_p}\right)^{\frac{3}{2}}, \; \alpha_p^2 = \sqrt{\frac{1-a}{2}}P \quad (34)$$

For large momentum P we find that ϕ^+ is quite flat in k, while ϕ^- is almost negligible,

$$\phi^- \simeq \frac{a}{2p}\Delta\phi^+ \,. \qquad (35)$$

This result is consistent with the relativistic space contraction. We checked that the components that we neglected here would yield a small contribution to the f_0 decay.

E. The coupling of a scalar to a pair of pseudoscalars

The form factor $F(P)$ for the coupling of a scalar f_0 to a pair of π can be decomposed in diagrams where a quark (antiquark) line either emits (absorbs) a pseudoscalar or a scalar. We use the truncated Bethe-Salpeter amplitude χ, as an intermediate step to compute the coupling of a

meson to a quark line $u^\dagger \chi u$. $F(P)$ is represented with a large triangle and the boundstate amplitudes χ and ϕ are represented with small triangles,

$$(36)$$

This includes the $q\bar{q}$ pair creation or annihilation of Fig. 2. The same irreducible interaction for quarks which is used in the boundstate equations is also [26] used for the annihilation. In eq. (36) the loop energies are trivial, see for instance eq. (A3), and we now compute the *momentum ⊗ spin* contribution.

We first consider the limit of a coupling to pions of low momentum P. The coupling of the pseudoscalar to the quark is derivative and thus is suppressed. For instance in the case of a massless π in the center of mass, using the wave-function of eq. (26), we find that

$$\chi = \left[-(1 - 3a)\sqrt{2}\mathcal{N}_p^{-1}\,\Delta\,(S) \right] \beta\gamma_5 + o(P)$$
$$\Rightarrow u^\dagger(k)\chi(k, 0)u(k) = o(P) , \qquad (37)$$

which is consistent with the derivative coupling of a pion to a quark. The dominant contribution includes the coupling of the $^3P_0$ scalar meson to the quark (antiquark) line. The coupling $F(P)$ to a pair of pions with low momentum P is,

$$F = tr \int \frac{d^3k}{(2\pi)^3} \phi^{-\dagger}\left(u^\dagger\chi_s u\phi^+ + \phi^+ v^\dagger\chi_s v\right) \qquad (38)$$

where for instance we get for the scalar coupling $u^\dagger(k)\chi_s(k)u(k)$ to the quark line,

$$u_{s_1}^\dagger\chi_s(k)u_{s_2} = \frac{\delta_{s_1 s_2}}{2\sqrt{2}}\left[(1 - a)C\hat{k}\cdot\Delta(\hat{k}Sk\phi_s)\right.$$
$$\left. -(1 - 3a)S\Delta(Ck\phi_s)\right] \qquad (39)$$

except for the $-i$ factor which goes with any potential insertion according to the Feynman rules. We will discard it in this section. Integrating by parts the eq.(38) can be simplified with the help of the mass gap equation and we get,

$$F = \int \frac{d^3k}{(2\pi)^3}\frac{k\phi_s}{\sqrt{2}}\left[-kS + \dot{\varphi}\frac{d}{dk} + aSC\Delta\right]\left(\phi^{-\dagger}\phi^+\right)$$
$$= \frac{0.011K_0^2 - 0.052M^2(P)}{f_\pi^2 M(P)}K_0^{1/2} . \qquad (40)$$

This coupling is very sensitive to the pion decay constant f_π and to the energy $M(P)$ of the pion.

We now consider the opposite limit of large pion momentum P. In this case the negative energy component of the pion is quite small. We expect that the dominant diagrams are the ones of the first line of eq. (34), which include only the positive energy ϕ^+. This is present in either the coupling of a pion to the quark line, or the coupling of a π to an antiquark line,

$$F(P) = \int \frac{d^3k}{(2\pi)^3}\phi_s(k_1, 0)(-\Delta'_k)\Big[\phi_p(k', P)\phi_p(k, -P)t_q$$
$$\left. +\phi_p(k, P)\phi_p(k', -P)t_{\bar{q}}\right]\Bigg|_{k'=k} , \qquad (41)$$

where t_q and $t_{\bar{q}}$ are respectively the traces in Dirac indices,

$$t_q = tr\left\{\frac{-i\sigma_2}{\sqrt{2}}\vec{\sigma}\cdot\vec{k}_1 u^\dagger(k_1)\Omega_l u(k'_1)\frac{i\sigma_2}{\sqrt{2}}v^\dagger(k'_2)\Omega_l u(k_2)\frac{i\sigma_2}{\sqrt{2}}\right\}$$
$$= tr\left\{\frac{\vec{\sigma}\cdot\vec{k}_1}{\sqrt{2}}\frac{(1 + \beta)}{2}\frac{(1 + \vec{\alpha}\cdot\hat{k}_1)}{\sqrt{2}}\Omega_l\frac{(1 + \vec{\alpha}\cdot\hat{k}'_1)}{\sqrt{2}}\right.$$
$$\left.\frac{1}{\sqrt{2}}\frac{(1 + \beta)}{2}\gamma_5\frac{(1 - \vec{\alpha}\cdot\hat{k}'_2)}{\sqrt{2}}\Omega_l\frac{(1 + \vec{\alpha}\cdot\hat{k}_2)}{\sqrt{2}}\frac{1}{\sqrt{2}}\right\} \qquad (42)$$

and $t_{\bar{q}}$, of the second diagram , with the coupling of the pion to the antiquark yields the same result. The total coupling is a functional of the scalar and pseudoscalar wavefunctions, which are described in eqs. (25,34) by Gaussians. We now apply the Laplacian to the functions of k'. The dominant term of the expansion in $2/P$ comes from the derivatives of ϕ_P. A derivative of $\phi_P(k', P)$ will be proportional to $P/2$ when the Gaussian integral is performed , while a derivative of t_q or $t_{\bar{q}}$ which are functions of respectively $\hat{k}'_1$ or $\hat{k}'_2$ is proportional to $1/P$ and will not produce a dominant term. The traces then simplify to,

$$t_q = t_{\bar{q}} = a\,\frac{k_1}{\sqrt{2}}\left[1 - (\hat{k}_1\cdot\hat{k}_2)^2\right] \qquad (43)$$

We now apply the Laplacian to ϕ_P, and expand the $\hat{k}_1\cdot\hat{k}_2$ in a series of $1/P$. It is convenient to define $\alpha_T^2 = 2\alpha_s^2 + \alpha_p^2$, and we get finally find for the *momentum ⊗ spin* contribution,

$$F(P) = \left[a\frac{-64\pi^{\frac{3}{4}}\ \alpha_s^{\frac{1}{2}}\alpha_p^2}{3^{\frac{1}{2}}\ (\alpha_p^2 + \alpha_T^2)^2\alpha_T^3}\frac{P}{2} + o\left(\frac{2}{P}\right)\right]e^{-\frac{(\frac{P}{2})^2}{\alpha_T^2}} \qquad (44)$$

where the dominant term is the a term which is of the order of $0.43\,K_0^{-1/2}$ for P of the order of $2K_0$.

The color factor for f_0 and π color singlets is $1/\sqrt{3}$. The flavor factor for the coupling of a scalar isosinglet $(u\bar{u} + d\bar{d})/\sqrt{2}$ to a pair of pseudoscalar isovectors, say $u\bar{d}$ and $-d\bar{u}$, with a flavor independent quark-antiquark annihilation is $-1/\sqrt{2}$. The total coupling is then $-F(P)/\sqrt{6}$.

The function $F(P)$ is very cumbersome to derive in the case of intermediate momenta. For momenta of the order of K_0, see Fig. 7, matching the high and low P limits with an interpolating function is a possible approximation.
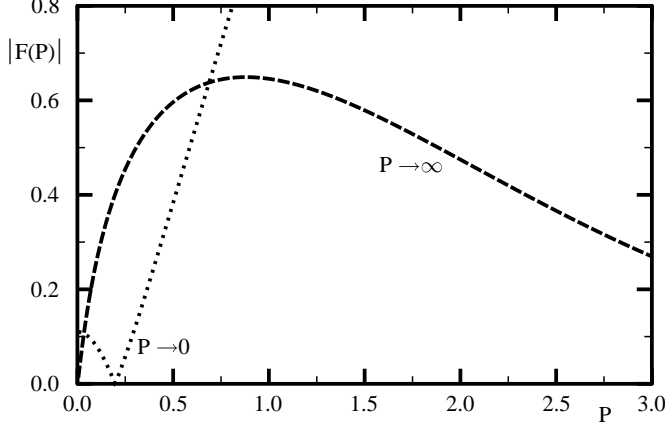

FIG. 7. We show $F(P)$, in the adimensional units of $K_0 = 1$. The dotted line and dashed line correspond respectively low P and high P limits.

F. The $f_0(980) \to \pi\pi$ decay

The decay width of a f_0 in a pair of π can be calculated from the the Breit-Wigner pole in the meson propagator. We call bare the ladder meson, see eqs. (7), (C1) and (C13). The bare mass M_0 is real and is a solution of the Bethe-Salpeter equation. When coupled channels of mesons are included, the bare meson is dressed. The dressed pole is composed by the bare mass M_0 plus the coupled channel contribution which includes a real mass shift, and an imaginary term in the case where the mass is above the coupled thresholds. The mass is then,

$$M = M_0 + \Delta M , \quad \Delta M = -i\Sigma$$

$$(45)$$

where we only included a loop of bare π, which is the simplest contribution to the scalar self energy. The integral in the loop energy provides an extra $2\pi i$ factor, which verifies that in general ΔM includes a real component, and we find that,

$$\Delta M = 6 \int \frac{d^3q}{(2\pi)^3} \frac{\frac{F(q)^*}{\sqrt{6}} \frac{F(q)}{\sqrt{6}}}{M_{f_0} - 2\sqrt{q^2 + M_\pi^2} + i\epsilon} \qquad (46)$$

where the factor of 6 includes the 3 different flavors of the isovector π, and the factor 2 from the direct and exchange diagram of the self energy in eq. (45). In this section we represent as usually the width of a resonance by a Γ, which should not to be confused with the same

symbol which is used in other sections for the vector or axial vertices. The width Γ is a simple function of the imaginary component of ΔM,

$$Im(\Delta M) = -i\frac{\Gamma}{2} , \quad \Gamma = \frac{1}{4\pi} P M_{f_0} |F(P)^2| \qquad (47)$$

where $P = \frac{1}{2}\sqrt{M_{f_0}^2 - 4M_\pi^2}$ is the momentum of the emitted π. Let us consider the case of a scalar mass M_{f_0} of the order of $1\,GeV$, where P is larger than the scale of the interaction by a factor of 1.4. In this case, it is sensible to use the limit of large momentum P for $F(P)$, see eq. (44). We finally find a partial decay width of just $40\,MeV$ for $F_0 \to \pi\pi$ which lies within the experimental limits. We expect that a complete calculation without the large P approximation would not deviate from this by more than a factor of 2.

This is also compatible with the narrow resonances $f_0(1500)$ and $a_0(980)$ which are possible groundstates. Concerning $K_0^*(1430)$ which is wider and has decay products with a larger momentum P, the function $\Gamma(P)$ of eq.(47) has the correct qualitative behavior of being proportional to P^3 for intermediate momenta. However in this model the exponential decrease is too strong, and the model needs some improvement in order to reproduce the correct $K_0^*(1430)$.

III. GOING BEYOND BCS WITH FINITE COUPLED CHANNEL EFFECTS

A. The Mass Gap Equation and the self energy

We find in Appendix D that the minimal extension of the mass gap equation beyond BCS is achieved with a new tadpole term in the self energy,

$$(48)$$

where the sub-diagram $\mathcal{O}$ is defined as an intermediate step. This amounts to extend the MGE for the self energy of the quarks with the simple one meson exchange. Using the Weyl fermions, and expanding the ladder in meson poles, we find that the self energy of the quark (antiquark) has a diagonal component Σ_d which contributes to the dynamical mass of the quark (antiquark),

$$(49)$$

9

and the energy of 1 quark is identical to the BCS one of eq. (18) except for the expected changes of the chiral angle φ. In eq.(49) we only included the nonvanishing diagrams which remain from an expansion in powers of $1/U$. The free Green functions are proportional to U^{-1}. The interactions without a pair creation or annihilation are proportional to the infinite infrared constant U, while the remaining interactions are finite. It turns out that the new coupled channel diagrams vanish. This happens because in the limit of an infinite $-U$ the box diagrams in eq. (48) which contribute to the quark energy vanish. This is the case for instance of diagrams (a) (c),

$$\cdots = 0, \quad \cdots = 0, \quad \cdots = \cdots \quad (50)$$

$$(a) \qquad\qquad (b) \qquad\qquad (c)$$

We find that the quark energy $E = E_0 - \Sigma_d$ remains the BCS one of eqs. (15) to (18),

$$E(k) = u^\dagger(k)\vec{\alpha}\cdot\vec{k}u(k) - \frac{1}{2}\Big\{ u^\dagger(k)\int\frac{d^3k'}{(2\pi)^3}V(k-k')$$
$$\Omega_l\Big[\Lambda^+(k') - \Lambda^-(k')\Big]\Omega_l u(k)\Big\}\,. \quad (51)$$

However the last diagram of eq. (50), which contributes to the mass gap equation is finite.

The mass gap equation is obtained when we impose that the antidiagonal components Σ_a of the self energy must cancel. As in eq.(15) this component in obtained with the projection of the spinors $u^\dagger$ and v. This produces a function Σ_a with the quantum numbers of a scalar, see eqs. (19) and (21). In order to use the results of the preceding section, it is convenient to fold Σ_a with a generic scalar wave function $\phi_{f_0}^+$. Then the resulting product must vanish for any $\phi_{f_0}^+$. In fact this ensures vacuum stability since this prevents the vacuum to decay in scalar modes. The diagrams that contribute to the antidiagonal component of the self energy in the mass gap equation are now,

$$tr\left\{\phi_{f_0}^+(k)^\dagger\Sigma_a\right\} = \quad + \quad$$

$$+ \qquad + \qquad$$

$$+ \qquad + \qquad . \quad (52)$$

In eq.(52) we only show the diagrams which are nonvanishing in orders of $1/U$, and in fact they all are finite,

of order U^0. The first pair of diagrams are BCS diagrams. It turns out that the new diagrams are the same diagrams which contribute to the $f_0 \rightarrow \pi\otimes\pi$ coupling, except for the negative energy wave function of the π and for the integral in the π momentum P. The negative energy wave-function ϕ^- always vanishes for high momentum P and in the case of low momentum P it is relevant only and for the pseudoscalar family of the π. We suppose that the large number of excited states is not sufficient to compensate the smallness of ϕ^-, and we will not consider this ultraviolet problem. Thus we will only include the coupled channel contribution of the π family. In the case of low momentum, the π family has a extremely large ϕ^-, however the coupling to a quark $u^\dagger\chi u$ is derivative and vanishes. This prompts us to neglect the last line of eq.(52). Finally we can remove, with a functional derivative, the variational scalar wave function $\phi_{f_0}^+$. The result after integrating in all the loop energies can be represented,

$$\Sigma_a = \tfrac{1}{2} \quad + \quad \tfrac{1}{2} \quad$$

$$+ \qquad + \qquad , \quad (53)$$

where the lines ___ only represent the spinors u, v, $u^\dagger$ or $v^\dagger$, the integrals and the traces and no longer include the quark or anti-quark propagators. The mass gap equation $0 = S_0^{-1}{}_a - \Sigma_a$ is now,

$$0 = +u_{s_1}^\dagger(k)\vec{\alpha}\cdot\vec{k}v_{s_5}(k)$$

$$-\Big\{u_{s_1}^\dagger(k)\int\frac{d^3k'}{(2\pi)^3}V(k-k')\Omega_l\Big[$$

$$+u_{s_2}(k')\Big(\frac{\delta_{s_2s_4}}{2} - \int\frac{d^3P}{(2\pi)^3}\phi_{s_2s_3}^-(P,k'-P/2)$$

$$\phi_{s_3s_4}^-{}^\dagger(P,k'-P/2)\Big)u_{s_4}^\dagger(k')$$

$$-v_{s_2}(k')\Big(\frac{\delta_{s_2s_4}}{2} - \int\frac{d^3P}{(2\pi)^3}\phi_{s_2s_3}^-{}^\dagger(P,k'-P/2)$$

$$\phi_{s_3s_4}^-(P,k'-P/2)\Big)v_{s_4}^\dagger(k')\Big]\Omega_l v_{s_5}(k)\,, \quad (54)$$

where the sum over repeated spin indexes s_i is assumed.

B. Model independent effects of the coupled channels

The dominant effect of coupled channels is to multiply the potential term in the mass gap equation by a factor

of ,

$$1 - 2 \int \frac{d^3 P}{(2\pi)^3} \phi_p^- \phi_p^{-\dagger} . \tag{55}$$

This clearly decreases the term which is the source for the spontaneous breaking of chiral symmetry. Thus the coupled channel effect is to restore partially the chiral symmetry. This effect is independent of the quark-quark interaction.

The signs of the new terms in the mass gap equation deserve a special attention since they determine whether the coupled channel effect will increase or decrease the chiral condensation. Because the coupled channel terms introduce in the mass gap equation a new fermion loop it is natural for Dirac Fermions that the coupled channel terms should be affected with a $-$ sign.

When the Dirac fermions are translated into Weyl fermions the quarks divide into the species of quarks and antiquarks which have independent field operators and propagators, and the $-$ signs are transfered from the propagator and the loops into the antiquark vertex and the exchange diagrams, and loops with quarks (antiquarks only). In this case we check with Weyl fermions that the $-$ sign persists and is due to the quark (antiquark) exchange. Only retardation, which was not included here, might perhaps oppose to this negative sign.

This sign can also be understood from the perspective of the Mexican hat potential $-\lambda \sigma^2 + \mu \sigma^4$ of effective meson models. In this case the quadratic term spontaneously creates a scalar condensate, while the quartic term opposes to the condensation and the actual condensate corresponds to the minimum of the energy density where the two terms are balanced. In the present paper there are three terms, a kinetic term which opposes to the condensate (and has no correspondence in the effective meson models) a BCS term which spontaneously breaks chiral symmetry (it is equivalent to the quadratic term of effective meson potentials) and a beyond BCS term which is equivalent to the quartic term in effective meson potentials. This correspondence, which is supported by the mean field theory where $\langle \bar{\psi}\psi \rangle \simeq \sigma$, confirms the negative sign of the coupled channel term. Thus we may assume quite generally that coupled channels oppose to the breaking of chiral symmetry.

An interesting feedback from chiral symmetry to the narrow width the groundstate occurs. Chiral symmetry breaking can be understood variationally, the solution $\varphi(k)$ of the mass gap equation also minimizes the energy density $\mathcal{E}$ of the vacuum. $\mathcal{E}$ is the sum of three terms, the free one, the BCS one and the beyond BCS one. Only the BCS term is negative and drives $\varphi(k)$ away from the trivial vanishing solution. The actual solution $\varphi(k)$ minimizes the free term *and minimizes the beyond BCS term* and at the same token produces the most negative BCS term. In eq.(52), we saw that the beyond BCS diagrams in the mass gap equation are similar to the diagrams of coupling of a scalar to a pair of pseudoscalars (with low

to moderate momentum). Thus we conclude that this coupling is naturally suppressed and that this suppression is selective in the sense that it is not supposed to occur in other hadronic couplings. This has an amplified effect in the scalar width which is a function of the square of this coupling.

C. Solution of the mass gap equation

We will now focus on the dominant terms among the coupled channel contributions, We obtain the $momentum \otimes spin$ coupled channel contribution,

$$\xi = \int dP dw \frac{-2P^2 \phi^-(k + P/2)\phi^-(k + P/2)^\dagger}{(2\pi)^2} \tag{56}$$

From the eqs. (26,34) we get for the the integrand of eq. (56),

$$P \to 0 , \quad -0.14 \frac{P^2}{M(P)} \left[S(k_1) - M(P)\frac{f_1(k_1)}{k_1} \right]^2 ,$$

$$P \to \infty , \quad -1.9 \frac{a^2 P^{5/4}}{(1-a)^{11/4}} e^{-k_1^2/\alpha_p^2} , \tag{57}$$

where the spin factor $\frac{i\sigma_2}{\sqrt{2}} \frac{-i\sigma_2}{\sqrt{2}} = \frac{1}{2}$ is included. The integral that leads to ξ is now evaluated with an interpolation between the two limits of eq(57), see Fig. 8. Because this interpolation is arbitrary, we have to include in the result a theoretical error.
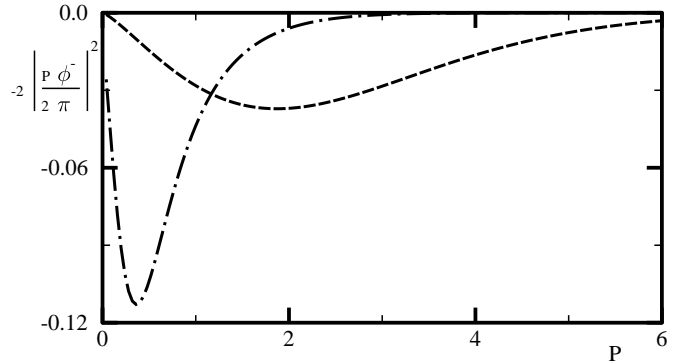

FIG. 8. We show the integrand of $\xi(0)$, in the adimensional units of $K_0 = 1$. The dotted line and dashed line correspond respectively to the cases where ϕ is obtained in the low P limit and in the high P limit.

We obtain the $momentum \otimes spin$ coupled channel contribution,

$$\xi(k) = -(0.4 \pm 0.1)S \tag{58}$$

which turns out to have a shape very close to the function $S = sin(\phi)$ which was evaluated at the BCS level. We estimate that the coupling to the quasi Goldstone bosons, including the momentum, spin, color and flavor contributions yields,

11

$$\xi(k) \simeq -(0.4 \pm 0.1)\, S \frac{1}{3}\left(N_f - \frac{1}{N_f}\right)$$
$$\simeq -(0.3 \pm 0.2)S \ , \quad N_f = 2 \to 3 \ . \tag{59}$$

N_f is the number of almost massless quark flavors which empirically is between 2 and 3.

The mass gap equation can be solved for a coupled channels contribution equal to ξ, when $\xi \geq -1$,

$$0 = u^\dagger \left[\vec{\alpha} \cdot \vec{k} - \frac{1}{2}\Omega_l \int V(\Lambda^+ - \Lambda^-)(1+\xi)\Omega_l \right] v \tag{60}$$

$$= \left\{ kS - [1 - a(2C^2 + 1)]\left[\frac{\Delta\varphi}{2}(1+\xi) + \dot{\xi}\dot{\varphi}\right] \right.$$

$$\left. -SC\left[\frac{1}{k^2} + a\left(\dot{\varphi}^2 - \frac{1}{k^2}\right)\right](1+\xi) + aSC\Delta\xi \right\}\vec{\sigma}\cdot\hat{k}i\sigma_2$$

The solution φ for $\xi = -0.3\, S_{BCS}$ is shown in Fig. 5. In this case and for the same parameter K_0, quark condensate $\langle\bar{\psi}\psi\rangle$ is decreased by a factor of $(1-0.12)^3$.

IV. RESULTS AND CONCLUSION

We developed a general formalism to include both the effects of chiral symmetry breaking and strong hadron-hadron interactions in quark models. This is encouraging since both effects are firmly established in phenomenology. We find new general effects in the scalar meson width, in the breaking of chiral symmetry and in the mass shifts of the hadron spectrum. Quantitative results are computed within a model which belongs to a class of Nambu and Jona Lasinio absolutely confining instantaneous interactions, in the case where the coupled pair of mesons are accounted as bare mesons.

We find in this model that the mass and width of the light $q\bar{q}$ scalar f_0 meson are close [11] to the experimental mass and width of the $f_0(980)$, and not to the $f_0(400-1200)$ or the $f_0(1370)$. This apparently indicates a possible solution to the scalar meson puzzle without meson molecules, glueballs or strongly nonlinear coupled channel effects. In this case the attraction which is visible in $\pi\pi$ phase shifts and in the intermediate range NN interactions would need other interpretations [27] than the very wide σ meson.

Compared with χSB at the BCS level, a new parameter has been identified, which leads to the percentage of coupled channel effects in the mass gap equation. We find that coupled channels suppresses the breaking of chiral symmetry. This results are model independent. With our model we get a suppression of the quark condensate by $5\% \to 55\%$ when the coupled channel effects are included.

We find a new interesting feedback mechanism from chiral symmetry to coupled channels and explain it variationally. The chiral symmetry restoring contribution to the mass gap equation from coupled channels is closely related to the coupling of a scalar to a pair of pseudoscalars. The feedback enforces that the width of a groundstate scalar decaying to a pseudoscalar pair (with low or moderate momentum) is reduced when compared to the width of any other resonance. This effect is model independent and contributes to understand the scalar meson puzzle.

Concerning real mass shifts we estimate that they are canceled due to the new terms which are introduced by the Ward Identities. This might improve previous [4,12] coupled channel calculations where this cancellation was not explicitly included. An systematic shift of the hadron spectrum is not expected. In this sense we agree with the results of Geiger and Isgur [28]. Nevertheless mass splittings between states with different quantum numbers are still expected from the boundstate equation. Different theoretical problems that could be reviewed with these new techniques are the contribution of the coupled channels to the hadron spectra, for instance to the interesting η' mass or to the N mass.

We conclude that in general the results of this paper, without ruling out other perspectives, explain why the simpler quark model is so successful.
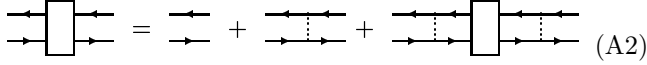
APPENDIX A: CONFINEMENT WITH INFRARED FINITE COUPLED CHANNELS

At the BCS level, the boundstates are obtained with the ladder approximation which is equivalent to the Salpeter equation, and to the Schrödinger equation (see Appendix C). In this case the infinite infrared divergent constant U of the interaction (3,4) is extremely convenient [22] to remove the colored states, which have masses proportional to U. Let us consider the dominant terms in orders of U of the energy of a system of n quarks and antiquarks. The 1-body energy includes the self energy (18) which is calculated with the Schwinger Dyson equation,

$$\sum_i E_i + \sum_{i<j} V_{ij} \simeq \frac{3}{4}\left(\frac{U}{2}\sum_i \frac{\vec{\lambda}_i}{2}\cdot\frac{\vec{\lambda}_i}{2} + U\sum_{i<j}\frac{\vec{\lambda}_i}{2}\cdot\frac{\vec{\lambda}_j}{2}\right)$$

$$\simeq \frac{3}{32}U\vec{\Lambda}\cdot\vec{\Lambda} \ , \tag{A1}$$

where $\vec{\Lambda}$ is the Gell Mann matrix of the total color of the system. The energy (A1) vanishes for color singlets only, thus colored states have an infinite energy and are confined.
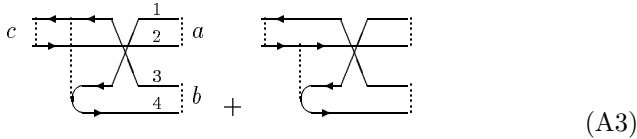
To include coupled channels in the energy of a color singlet, for instance in a meson, we consider the complete series of diagrams that contribute to the irreducible $q\bar{q}$ interaction. One has to include all the possible number of quark loops and all the possible insertions of the microscopic quark-quark interaction. Then this series can be resumed in order to factorize the bare meson ($q\bar{q}$) and hadron (qqq) ladders. According to Appendix C, the ladder needs integrals $\int \frac{dw}{2\pi}$ in all the external relative energies in order to have a hadron pole. To ensure in a particular diagram that the meson poles are present it is convenient to decompose the ladder in,

$$(A2)$$

where in the right hand side the ladder is integrated and contains the meson pole, and the first pair of diagrams contributes to the overlap interactions of hadrons. In order to simplify the calculations it is convenient to truncate eventually the series of diagrams. The pertubative parameter is then the number of considered ladders. This is both straightforward and also close to the hadronic phenomenology.

We now show how the interactions of color singlet ladders can be finite, when they are built from the infrared divergent quark-quark microscopic interaction (4), and the quark propagators are divergent as well. When a hadron is emitted or absorbed we have quark-antiquark annihilation overlaps, for instance in a 3-meson vertex,
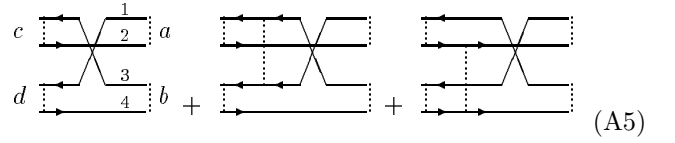

$$(A3)$$

We first integrate the relative energies in the first diagrams of q. (A3),

$$\int \frac{dw\,dw'}{(2\pi)^2} \frac{i}{w - E_1 + i\epsilon} iV_{1\bar{4},3} \frac{i}{-w' - E_4' + i\epsilon}$$
$$= \frac{i}{w' - E_3' + i\epsilon} \frac{i}{w - E_3 + i\epsilon} \frac{i}{-w - E_2 + i\epsilon}$$
$$= -iV_{1\bar{4},3} G_{0a} G_{0b} G_{0c} \ . \tag{A4}$$

where the G_{0n} are in fact part of the respective BS amplitudes which are untruncated. The remaining factor $-iV_{1\bar{4},3}$ is finite because the term proportional to U in the quark-antiquark annihilation vertex is $v_s^\dagger(k)\delta^3(k-k')u_{s'}(k') = 0$.

When the number of hadrons are conserved, this is the case in elastic scattering, we have quark exchange overlaps, for instance in a 4-meson vertex,

$$(A5)$$

The integrals in the relative energies are,

$$\int \frac{dw}{2\pi} \frac{i}{w - E_1 + i\epsilon} \frac{i}{-w - E_4 + i\epsilon} \frac{i}{w - E_3 + i\epsilon} \frac{i}{-w - E_2 + i\epsilon}$$
$$= i(E_1 + E_2 + E_3 + E_4) G_{0a} G_{0b} G_{0c} G_{0d}$$
$$\int \frac{dw\,dw'}{(2\pi)^2} \frac{i}{w - E_1 + i\epsilon}(-iV_{13}) \frac{i}{w' - E_1' + i\epsilon}$$
$$\frac{i}{-w' - E_4' + i\epsilon} \frac{i}{w' - E_3' + i\epsilon} \frac{i}{w - E_3 + i\epsilon} \frac{i}{-w - E_2 + i\epsilon}$$
$$= -iV_{13} G_{0a} G_{0b} G_{0c} G_{0d} \ . \tag{A6}$$

The four G_{0n}, will be absorbed by the Salpeter amplitudes and the remaining factors are,

$$i(E_1 + E_2 + E_3 + E_4 - V_{13} - V_{24})P_{13}$$
$$= i(E_1 + E_2 + E_3 + E_4 + V_{14} + V_{23})P_{13}$$
$$= iP_{13}(E_1 + E_2 + V_{12} + E_3 + E_4 + V_{34})$$
$$= iP_{13}(0U + \ldots) \tag{A7}$$

where the infinite $-U$ terms cancel in the same way as in eq. (A1) because the mesons $_{32}$ and $_{14}$ in the left and $_{12}$ and $_{34}$ in the right are color singlets. We find that all the terms proportional to U cancel when the complete set of diagrams which contribute to the interaction between color singlets is included.

In this framework the masses of bare hadrons and their interactions are finite and can be evaluated. Then we compute the masses and widths of dressed hadrons. These are the final freedom degrees which can be compared with the experimental spectrum of hadronic resonances.

APPENDIX B: THE LIGHT π AND WARD IDENTITIES

The solution to the pion mass problem is found using [20,29] the Ward identities (WI) in order to insure that the bound state equation for the pion -a Bethe Salpeter equation with coupled channels - is consistent with the non linear mass gap equation. The WI were first derived for fermion-gauge field theories, and were initially based on the simple observation that for free fermions with propagator $\mathcal{S}_0(p) = \dfrac{i}{\not{p} - m_0}$ and a free vector vertex $\Gamma_0^\mu = \gamma^\mu$,

$$i(p_\mu - p_\mu')\mathcal{S}(p)\Gamma^\mu(p,p')\mathcal{S}(p') = \mathcal{S}(p) - \mathcal{S}(p') \tag{B1}$$

The difference in the right member of the equation extends the identity to renormalized propagators and vertices. This identity is then crucial for the conservation

of electric charge. The WI enforce that the self energy of the MGE is obtained (without double-counting) from the BS kernel by closing the fermion line where the vertex is inserted. Inversely, they also ensure that the BS kernel is obtained if one inserts the vertex in all possible propagators of the self energy. For instance this mapping is trivial at the BCS level where the mass gap equation (5) is clearly equivalent to the bound state equation (6). Let us now consider a more general case, where the fermion self energy include a product of bare propagators $S_{\alpha_i\beta_i}(k_i + P)$. The external momentum is P and k_i is a loop momentum. The propagators can be factorized and we get,

$$\Sigma(P) = \cdots \prod_i S_{\alpha_i\beta_i}(k_i + P) \ . \tag{B2}$$

Then the vertex Γ can be constructed if we insert a bare vertex in all possible bare propagators, and we get,

$$\Gamma^\mu(P_1 - P_2) = \cdots \sum_j \prod_{i1 \leq j} S_{\alpha_{i1}\beta_{i1}}(k_{i1} + P_1)$$
$$\gamma^\mu \prod_{i2 \geq j} S_{\alpha_{i2}\beta_{i2}}(k_{i2} + P_2) \ . \tag{B3}$$

Inversely the original self energy can be recovered if we substitute the bare vertex by the difference of propagators,

$$i(P_{1\mu} - P_{2\mu})\Gamma^\mu = \cdots \sum_j \prod_{i1 < j} S_{\alpha_{i1}\beta_{i1}}(k_{i1} + P_1)$$
$$\left[S_{\alpha_j\beta_j}(k_j + P_1) - S_{\alpha_j\beta_j}(k_j + P_2)\right] \prod_{i2 > j} S_{\alpha_{i2}\beta_{i2}}(k_{i2} + P_2)$$
$$= [\Sigma(P_1) - \Sigma(P_2)] \tag{B4}$$

where the products which depend on both P_1 and P_2 cancel. and this removes the double counting.

There is also a WI identity for the free axial vector vertex $\Gamma_f^{\mu 5} = \gamma^\mu\gamma^5$ that involves the free pseudoscalar vertex $\Gamma_f^5 = \gamma^5$,

$$-i(p_\mu - p'_\mu)\mathcal{S}(p)\Gamma^{\mu 5}(p,p')\mathcal{S}(p')$$
$$+2im\mathcal{S}(p)\Gamma^5(p,p')\mathcal{S}(p') = \mathcal{S}(p)\gamma^5 + \gamma^5\mathcal{S}(p') \tag{B5}$$

which is valid in a renormalization program providing the interaction is chiral invariant. In this case an equation analogous with eq.(B5) is complied by the axial and pseudoscalar vertices and by the self energy.

A key product of the axial WI is the proof [7,30] that a pseudoscalar Goldstone boson exists when current quark are vanishing and chiral symmetry breaking occurs. The full propagator is then renormalized and the self-energy Σ has a mass-like term,

$$\mathcal{S}^{-1}(p) = \mathcal{S}_0^{-1}(p) - \Sigma(p) \ , \ i\Sigma = A(p) - \not{p}B(p) \ . \tag{B6}$$

$$\mathcal{S}^{-1}(p) = \mathcal{S}_0^{-1}(p) - \Sigma(p) = \frac{A(p)\not{p} - B(p)}{i} \ . \tag{B7}$$

If we substitute this propagator in the WI, we find the solution for the pseudoscalar vertex Γ^5 with a vanishing $p - p'$,

$$\Gamma^5(p = p') = \frac{B(p)}{m_0}\gamma^5 \tag{B8}$$

which diverges for a vanishing quark mass m_0 and shows that the pole of a massless pseudoscalar meson appears in the axial vector vertex, with a boundstate truncated amplitude of

$$\chi(p - p' \simeq 0) = \frac{B\gamma_5}{f_\pi} \tag{B9}$$

where f_π includes a norm. Incidentally, this identity also offers a proof of the Gell-Mann, Oakes and Renner relation. If we expand the vertex Γ^5 in the neighborhood of the π pole,

$$\Gamma^5 = \chi \frac{i}{(p - p')^2 - M^2} tr\left\{\chi\mathcal{S}(p)\Gamma_0^5\mathcal{S}(p')\right\} \tag{B10}$$

where we included the integral in the trace. substituting Γ_5 in eq. (B8) and performing a trace with $\mathcal{S}\gamma_5\mathcal{S}$, we find for small masses

$$tr\left\{\gamma_5 \frac{B\mathcal{S}\gamma_5\mathcal{S}}{f_\pi}\right\}\frac{i}{-M^2}tr\left\{\frac{B\mathcal{S}\gamma_5\mathcal{S}}{f_\pi}\gamma_5\right\} = tr\left\{\gamma_5\frac{B\mathcal{S}\gamma_5\mathcal{S}}{m_0}\right\}$$
$$\Rightarrow -m_0\, tr\{\mathcal{S}\} = -2m_0\langle\bar\psi\,\psi\rangle = M^2 f_\pi^2 \tag{B11}$$

In QCD it is necessary to include the axial anomaly, in the flavor singlet WI which corresponds to the η' channel. The flavored axial currents remain unchanged, in particular the π, K, η remain quasi Goldstone bosons. We will now simply assume that the η' is heavier [2,7,16,31] than the usual $N_f^2 - 1$ Goldstone bosons, where N_f is the number of light quark flavors.

APPENDIX C: THE SALPETER EQUATIONS IN THE ENERGY-SPIN FORMALISM

When the interaction is instantaneous, a simplification occurs in the Bethe-Salpeter S matrix in the ladder approximation,

$$\tag{C1}$$

The S matrix only has 4 independent sub-matrices, which have to be calculated iteratively. The other 12 sub-matrices are directly computed from the independent 4 ones. The Salpeter equations are obtained when all the relative quark-antiquark energies of the system (C1) are integrated,

$$\int \frac{dw}{2\pi} \frac{i}{w + W/2 - E_q + i\epsilon} \frac{i}{w + W/2 - E_{\bar{q}} + i\epsilon} = \frac{i}{W - E_q - E_{\bar{q}} + i\epsilon} , \tag{C2}$$

The Salpeter equations can then be written in the compact form,

$$S = G_0 + G_0 V S$$
$$\Rightarrow (G_0^{-1} - V)S = 1$$
$$\Rightarrow (W\sigma_3 - H + i\epsilon)S = i \tag{C3}$$

where σ_3 is the Pauli matrix,

$$S = \begin{bmatrix} S^{++} & S^{+-} \\ S^{-+} & S^{--} \end{bmatrix} ,$$
$$G_0 = \begin{bmatrix} \frac{i}{W - E_q - E_{\bar{q}} + i\epsilon} & 0 \\ 0 & \frac{i}{-W - E_q - E_{\bar{q}} + i\epsilon} \end{bmatrix} ,$$
$$V = -i \begin{bmatrix} \int V_d & \int V_a \\ \int V_a & \int V_d \end{bmatrix} ,$$
$$H = \begin{bmatrix} E_q + E_{\bar{q}} + \int V_d & \int V_a \\ \int V_a & E_q + E_{\bar{q}} + \int V_d \end{bmatrix} \tag{C4}$$

and it turns out that H is an hermitian and positive operator.

The Salpeter wave-functions are the solutions of the homogeneous equations,

$$(M\sigma_3 - H)\phi = 0 , \phi = \begin{pmatrix} \phi^+ \\ \phi^- \end{pmatrix} \tag{C5}$$

which is an eigenvalue equation, similar to the Schrödinger equation, except for the σ_3. This formalism is known as the energy-spin formalism, where ϕ^+ is called the positive energy wave-function and ϕ^- is called the negative energy wave-function. The Salpeter equation (C5) is equivalent to the variational equation,

$$\delta \left(\frac{\langle \phi | H | \phi \rangle}{\langle \phi | \sigma_3 | \phi \rangle} \right) = 0 , \tag{C6}$$

which suggests that a normalizing condition of the wave functions might be,

$$\langle \phi | \sigma_3 | \phi \rangle = |\phi^+|^2 - |\phi^-|^2 = 1 . \tag{C7}$$

Let us study the class of solutions ϕ_u where this norm is possible, i. e. $|\phi_u^+| > |\phi_u^-|$. Once the single quark energies E and the 2-quark diagonal V_d and antidiagonal V_a potentials are defined, the solutions can be obtained

numerically, either iteratively or variationally, and one finds a whole spectrum of solutions with energy $M > 0$. When M increases, we find that $|\phi_u^-|$ is proportional to M^{-1}, and in the limit of large mass we exactly recover Schrödinger equation. However another class of solutions ϕ_d is unavoidable, with a one to one correspondence with the ϕ_u, and where $|\phi_d^-| > |\phi_d^+|$,

$$\phi_d^+ = \phi_u^- , \phi_d^- = \phi_u^+ , M_d = -M_u$$
$$\langle \phi_u | \sigma_3 | \phi_u \rangle = 1 , \langle \phi_d | \sigma_3 | \phi_d \rangle = -1 \tag{C8}$$

thus the spectrum is unbound. Exactly half of the solutions have a negative mass and a negative norm. When we include the infinitesimal $i\epsilon$ in eq. (C5), we find that the larger component of ϕ dominates and the eigenvalues are now,

$$M_u \to M_u - i\epsilon$$
$$M_d \to M_d + i\epsilon = -(M_u - i\epsilon) \tag{C9}$$

The operators H and σ_3 are both hermitian, thus the set of solutions $|\phi\rangle$ constitute a basis of the Hilbert space, orthogonal in the sense that $\langle \phi | \sigma_3 | \phi' \rangle = 0$, and the identity element is,

$$1 = \sum \frac{\sigma_3 |\phi\rangle\langle\phi|}{\langle\phi|\sigma_3|\phi\rangle} = \sum_u \sigma_3 |\phi\rangle\langle\phi| - \sum_d \sigma_3 |\phi\rangle\langle\phi| \tag{C10}$$

Inserting this partition in the S matrix equation (C3), we find,

$$i = (W\sigma_3 - H)S$$
$$= \sum \frac{\sigma_3|\phi\rangle\langle\phi|}{\langle\phi|\sigma_3|\phi\rangle}(W\sigma_3 - H + i\epsilon)\sigma_3 \sum \frac{\sigma_3|\phi\rangle\langle\phi|}{\langle\phi|\sigma_3|\phi\rangle}\sigma_3 S$$
$$= \sum \sigma_3|\phi\rangle \frac{W - M + i\epsilon\langle\phi|\sigma_3|\phi\rangle}{\langle\phi|\sigma_3|\phi\rangle}\langle\phi|\sigma_3 S$$
$$\sigma_3 S = \sum \sigma_3|\phi\rangle \frac{i\langle\phi|\sigma_3|\phi\rangle}{W - M + i\epsilon\langle\phi|\sigma_3|\phi\rangle}\langle\phi|$$
$$S = \sum_u |\phi_u\rangle \frac{i}{W - M_u + i\epsilon}\langle\phi_u|$$
$$- \sum_d |\phi_d\rangle \frac{i}{W - M_d - i\epsilon}\langle\phi_d| \tag{C11}$$

and the states with negative energy and negative norm can be reinterpreted as boundstates with positive mass moving forward in time, where the variable $W = P_0$ in the propagator turns out to be negative,

$$S = \sum_u |\phi_u\rangle \frac{i}{W - M_u + i\epsilon}\langle\phi_u|$$
$$+ \sigma_1 |\phi_u\rangle \frac{i}{-W - M_u + i\epsilon}\langle\phi_u|\sigma_1 \tag{C12}$$

and it suffices to work with the ϕ_u. Diagrammatically we get for instance,

$$\int \frac{dw\,dw'}{(2\pi)^2} \quad \boxed{++} \quad = \quad \text{(diagram with } E \text{)}$$

$$+ \quad \text{(diagram with } -E\text{)} \tag{C13}$$

where w and w' are the external energies. The quark antiquark BS amplitude is represented by the triangle ▷ and the boson propagator of the meson is represented by the double line ══. It is consistent to substitute the d wave-functions and masses in terms of the components ϕ_u^+, ϕ_u^- and the masses M_u. In the paper this reinterpretation will be assumed and we will skip the subindex u. The practical result is that we can use the amplitude ϕ^+ when the bra(ket) precedes(succeeds) the meson propagator, and we use the amplitude ϕ^- for the opposite case.

APPENDIX D: THE BETHE SALPETER EQUATION WITH COUPLED CHANNELS

We now go beyond BCS including the mesonic coupled channels both in the MGE and in the bound state equations. It is convenient to return to the Dirac formalism in order to reduce the number of diagrams when we apply the WI. We will extend the BS for the $q\bar{q}$ boundstate of the quarks with the minimal meson loop of coupled channels.

$$\bullet\!\!=\ =\ \Gamma_0\ +\ \text{(diagram)}\ +\ \text{(box diagram)}\ D \tag{D1}$$

where we follow the approximation of including only 3-legged effective meson vertices in the meson interaction. We will show that this is imposed by the box at the left of the beyond BCS diagram in eq. (D1). Upon iteration the equation,

$$\Gamma = \Gamma_0 + V\,G_0\,\Gamma + V\,G_0\,V\,M\Gamma \tag{D2}$$

can be resumed. If we factorize the S matrix at the ladder level $S_0 = (1 - G_0 V)^{-1} G_0$, see eq. (C3), the ladder will appear in the middle of the coupled channel terms,

$$G_0\,\Gamma = S_0\,\Gamma_0 + G_0 V\,S_0\,V\,M\Gamma\ ,$$
$$\Gamma \simeq V\,S_0\Gamma_0 + V\,S_0\,V\,M\Gamma. \tag{D3}$$

When the ladders S_0, including the two ones of the meson loop in M, are expanded in meson poles and wave functions according to eq. (C13), we recover the meson - meson pair coupling of eq. (36). The resulting pole of the vertex Γ is the mass of the dressed meson $M_0 + \Delta M$. This is equivalent to the Resonating Group Method equations [26] for coupled channels of one meson with a pair of non-interacting mesons.

We now use the WI prescription of removing the vertex and closing the respective fermion line to arrive at the mass gap equation (48). To recover the full vertex equation we must insert the vertex in all possible propagators of eq. (48). We then arrive at a WI consistent Bethe Salpeter equation for the vertex and for the boundstate,

$$\bullet\!\!=\ =\ \Gamma_0\ +\ \text{(diagram)}\ +$$

$$\text{(diagrams with } \mathcal{O}\text{)}\ +$$

$$\text{(more diagrams)}\ +$$

$$\text{(box diagrams)}\ +$$

$$\text{(box diagrams)}\ +$$

$$\text{(box diagram)} \qquad D \tag{D4}$$

where the diagrams are shown in separate lines according to their properties. Line 1 corresponds to the BS equation at the BCS level. Without the other lines it would reproduce the ladder Bethe-Salpeter equation for the vertex. The lines 2, 3 and 5 were separated because they contain all the contain terms proportional to the infrared divergent U, but they cancel in each line and all lines are finite. The remaining lines 4 and 6 contain the terms that one would except in coupled channel equations where a pair of mesons is created and then annihilated (except for the first diagram of line 4 which vanishes). With them we calculate for instance the partial decay width of a resonance into a channel of 2 mesons. The last lines 5 and 6 are only relevant for flavor singlets because the quark pair in the incoming meson is annihilated, thus for flavor vectors they are null.

The cancellation of the infrared divergences become clear in the Goldstone-Weyl formalism. Let us consider for instance the diagrams of line 2 in eq. (D4),

$$\text{(diagram with } -E\text{)}\ +\ \text{(diagram with } -E\text{)}\ +\ \text{(diagram with } -E\text{)} \tag{D5}$$

These 3 diagrams are infrared divergent but their sum is finite, in an analogous way to eq. (A5).

It is important to remark that in the previous calculations in the literature, the extrapolation from the ladder level to the coupled channel level would only include the diagrams of lines 4 and 6. We now find the previous choice arbitrary since the diagrams of lines 2, 3 and 5 were not considered. The role of these diagrams is to cancel any real mass shift of the π due to the usual coupled channel diagrams of lines 4 and 6, in order that the π remains a Goldstone boson in the chiral limit. This is ensured by the WI, see eq. (B8). Concerning widths, since the new diagrams are real, the results of the previous calculations in the literature are correct. However we find no systematic real mass shift in the meson spectrum due to coupled channels. This contradicts most of the real mass shifts of hundreds of MeV which are common in the literature. Only splittings between different levels, due to neighboring cuts, may be affected by coupled channels.

[1] Review of Particle Physics, Particle Data Group, Phys. Rev. D **54**,1 (1996).

[2] A. Szczepaniak, E. Swanson, C.-R. Ji and S. Cotanch, Phys. Rev. Lett. **76**, 2011 (1996).

[3] J. Weinstein, N. Isgur, Phys. Rev. Lett **48**, 659 (1982); Phys. Rev. D **27**, 588 (1983).

[4] E. Van Beveren, T. Rijken, K. Metzger, C. Dullemond, G. Rupp, J. Ribeiro Zeit. Phys. C **30**, 615 ,(1986).

[5] N. Törnqvist, M. Roos, Phys. Rev. Lett **76**, 1575, (1996); N. Tornqvist Zeit. Phys. C **68**, 647 (1995).

[6] J. Bardeen, L. N. Cooper and J. R. Schrieffer, Phys. Rev. **108**, 1175 (1957); L. V. Keldysh and A. N. Kozlov, Sov. Phys. JETP **27**, 521 (1968).

[7] Y. Nambu, G. Jona-Lasinio, Phys. Rev. **122**, 345 (1961); **124**, 246 (1961).

[8] F.T. Hawes and A. G. Williams, Phys. Lett. B **268**, 271 (1991); A. Bashir and M. R. Pennington, Phys. Rev. D **50**, 7679 (1994); H. J. Munczek, Phys. Rev. D **52**, 4736 (1995); A. Bender, C. D. Roberts, L. V. Smekal, Phys. Lett. B **380**, 7 (1996).

[9] P. Bicudo, preprint FISIST/5-97/CFIF and hep-ph/9703229 (1997).

[10] P. Bicudo and J. Ribeiro, Phys. Rev. D **42**, 1611 (1990).

[11] Y. le Yaouanc, L. Oliver, S. Ono, O. Pene and J.-C. Raynal, Phys. Rev. D **29**, 1233 (1984); Phys. Rev. D **31**, 137 (1985).

[12] P. Bicudo and J. Ribeiro, Phys. Rev. D**42**, 1635 (1990); P. Bicudo, J. Ribeiro and J. Rodrigues, Phys. Rev. C**52**, 2144 (1995); P. Bicudo and J. Ribeiro, Phys. Rev. C **55**, 834, (1997). P. Bicudo, L. Ferreira, C. Placido and J. Ribeiro, Phys. Rev. C **56**, 670, (1997).

[13] R. Friedrich and H. Reinhardt, Nucl. Phys. A**549**, 406 (1995); S. Gao, C. Shakin and W.-D. Sun, Phys. Rev. C **53**, 1374 (1996); K. Mitchel and P. Tandy, Phys. Rev. C **55**,1477 (1997); C. Shakin and W.-D. Sun, Phys. Rev. D **55**, 2874 (1997).

[14] S. Pepin, F. Stancu, M. Genovese, J. M. Richard, to be published in COMO2, world scientific, preprint nucl-th/9608058.

[15] A. Thomas and G. Miller, Phys. Rev. D **42**, 288 (1991).

[16] N. Törnqvist, preprint hep-ph/9612238 (1996); Phys. Lett. B**406**, 70 (1997); Phys. Lett B**426**, 115 (1998).

[17] J. E. Villate, D.-S. Liu, J. E. Ribeiro, P. Bicudo, Rev. D **47**, 1145 (1993).

[18] R. Cahill and C. Roberts, Phys. Rev. D **32**, 2419 (1985).

[19] Y. Dai, Z. Huang and D. Liu, Phys. Rev. D **43**, 1717 (1991).

[20] S. Adler and A. C. Davis, Nucl. Phys. B **224**, 469 (1984).

[21] Y. Kalinowsky, L. Kaslun, and V. Pervushin, Phys. Lett. B**231**, 288 (1989); R. Horvat, D. Kekez, D Klabucar and D. Palle, Phys. Rev. D **43**, 1585 (1991);

[22] P. Bicudo, G. Krein, J. Ribeiro and J. Villate, Phys. Rev. D**45**, 1673 (1992);

[23] P. Bicudo and J. Ribeiro, Phys. Rev. D**42**, 1625 (1990);

[24] P. Bicudo Phys. Rev. Lett. **72**, 1600 (1994).

[25] J. Lagae, Phys.Rev. D**45**, 317 (1992); A. Szczepaniak and E. Swanson, Phys.Rev. D**55** 3987 (1997); P. Bicudo, N. Brambilla, E. Ribeiro, A. Vairo, Phys. Lett. B**442** 349 (1998).

[26] Fujiwara and Hecht, Nucl. Phys. A451, 625 (1986);

[27] F. Wang, G. Wu, L. Teng, and T. Goldman, Phys. Rev. Lett. 69, 2891 (1992); Phys. Rev. C 53, 1161 (1996).

[28] P. Geiger and N. Isgur, Phys. Rev. D **44**, 799 (1991); Phys. Rev. Lett. **67**, 1066 (1991); Phys. Rev. D **47**, 5050 (1993).

[29] J. Schrieffer, " Theory of Superconductivity ", W. A. Bemjamin (1964);

[30] H. Pagels, Phys. Rev. D **14**, 2747 (1976).

[31] G. 't Hooft Phys. Rev. Lett. **37**, 8 (1976); Phys. Rev. D. **14**, 3432 (1976). V. Bernard, R. L.Jaffe, U.-G. Meissner, Nucl. Phys. B **308**, 753 (1988).